SYNOPTIC: Gyroscope in Torque-to-Balance Strapdown Application, J. P. Gilmore and J. Feldman, Charles Stark Draper Laboratory, Massachusetts Institute of Technology, Cambridge, Mass.; *Journal of Spacecraft and Rockets*, Vol. 7, No. 9, pp. 1076–1082.

Strapdown Gyroscope: Spacecraft Navigation Guidance and Flight Path Control Systems

Theme

Design factors associated with a single-degree-of-freedom gyroscope as applied to a strapdown guidance system are reviewed. The basic response of the gyro in the pulse-rebalance ternary digital torque-to-balance loop is discussed and multiple pulse-bursting phenomena are presented. A linearizing compensation technique is then described. Error sources associated with the torque generator are placed in perspective by consideration of the size 18 Inertial Reference Integrating Gyro (18 IRIG MOD B, Fig. 1 and Table 1). Specifically, a.c. torque sensitivity and scale-factor errors associated with float axial, radial and rotational displacement are reviewed. Test results illustrating stability, linearity, and error sensitivities are shown.

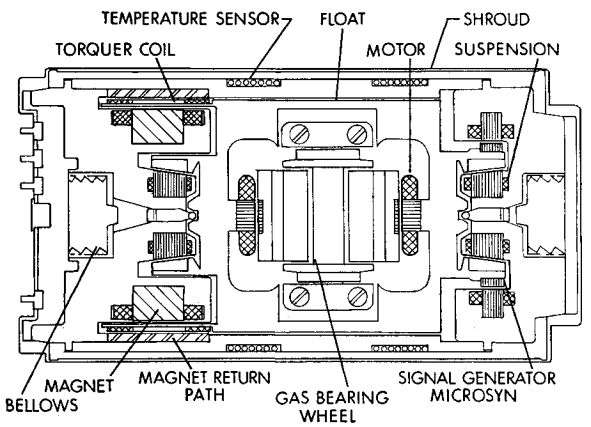

Fig. 1 18 IRIG MOD B Simplified cutaway view.

Content

Evaluation tests were conducted on an 18 IRIG MOD B, designed specifically for a strapdown environment. The torquer is compatible with input rates ≤ 1 rad/sec and the suspension design prevents radial side loading for rates somewhat in excess of 1 rad/sec. The gyro is operated in a closed loop, where by the torques on the float are restrained by control signals to the torque generator. Any rate about the input axis of the gyro produces a torque about its output axis and causes the float to rotate from a null position. The direction and magnitude of the float rotation is sensed by the signal generator (SG). When the SG output voltage reaches a given threshold level, a discriminator provides a positive or negative set signal, depending on the polarity of the SG output voltage. These set signals are interrogated at a given clock frequency to switch a control current of fixed amplitude and duration into the positive or negative direction of the torque-generator winding torque.

An interesting performance characteristic discussed, which is not a dynamic error, is the multiple-pulsing phenomenon that occurs when the gyro is operated in a pulse torque-to-balance control loop. Multiple-pulsing occurs because of the dynamic storage characteristics of the gyro float time constant. The float response shows that only a small percentage of the total float motion to a single fixed-magnitude torquing pulse occurs in the first sample period. For example, at a 9600-pulse/sec interrogation rate, the float has only begun to move when the torque pulse is turned off and has gone 11% of its commanded travel when the next torque-loop interrogation sample takes place. Clearly, at 9600-pulse/sec closed-loop operation, an angular rate about the gyro input axis that is in excess of 11% of the torque-loop full-on rate-scaling capability will result in some form of multiple-torquing pulsing. This moding and multiple pulsing is compensated for by a new technique which models the gyro so that the response of the gyro to the actual pulses issued is continuously developed. Float motion response to pulse commands is anticipated by first synthesizing a compensation signal based on the computed float response to each torque pulse and then comparing this signal to the actual float status. Float motion delays are thereby accounted for, and multiple pulsing is eliminated.

Table 1 18 IRIG MOD B nominal parameters and operational features

Angular momentum, H	0.145×10^6 g-cm²/sec
Output axis damping coefficient, C_{OA}	674,000 dyne-cm-sec
Output axis inertia, I_{OA}	225 g-cm²
Float time constant, $t_f = I_{OA}/C_{OA}$	334 μsec
Transfer function, HS_{SG}/C_{OA}	4.3 mv/mrad
Torquer rate scale factor, SF	1636°/hr-ma
Torquer time constant, $t_{tg} = L/R$	55 μsec
Anisoinertia coefficient $(I_{SA} - I_{IA})/H$	9.6°/hr/(rad/sec)²
Anisoelastic coefficient, K_{IO}	0.012°/hr-g²
Float mass unbalance uncertainty, ADIA, ADSRA	0.075°/hr-g

Effects of torquer geometry and material selection on performance sensitivities must be considered. Some of these sensitivities are identified for gyro rotational float angle, float radial and axial positions, magnet material interaction, and thermal inputs. Eddy current effects on scale factor linearity due to conductivity selection in the torquer assembly are highly significant. Similarly, precise torque-generator-to-signal-generator alignment is shown to have a direct influence on strapdown scale factor performance.

Performance on the order of 5 ppm for a 14-hr scale factor stability run (Fig. 2) and linearity on the order of 50 ppm for a ±25°/sec test range are demonstrated.

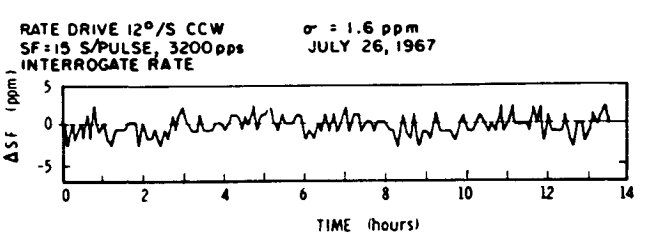

Fig. 2 Pulse torque SF Stability 18 IRIG MOD B 411.

Gyroscope in Torque-to-Balance Strapdown Application

JEROLD P. GILMORE* AND JULIUS FELDMAN†
Charles Stark Draper Laboratory, Massachusetts Institute of Technology, Cambridge, Mass.

Design factors associated with single-degree-of-freedom gyroscopes as applied to a strapdown guidance system are reviewed. The basic response of the gyro in the pulse-rebalance ternary digital torque-to-balance loop is discussed and multiple pulse-bursting phenomena are presented. A linearizing compensation technique is then described. Error sources associated with the torque generator are identified and placed in perspective by consideration of the size 18 Inertial Reference Integrating Gyro (IRIG), a single-degree-of-freedom gyro designed for strapdown application. Specifically, a.c. torque sensitivity and scale-factor errors associated with float axial, radial, and rotational displacement are reviewed. Test results illustrating stability, linearity, and error sensitivities are shown.

Introduction

THIS paper presents single-degree-of-freedom (SDF) gyroscope design factors that are applicable to its implementation in the strapdown guidance system. In a strapdown application the instrument encounters the full spectrum of vehicle dynamic environment. As a result, error sources considered to be of no consequence in stabilized platform applications must be evaluated. Similarly, design features of the gyroscope, particularly the torquer and the suspension, must be carefully evaluated relative to the strapdown environment.

The dynamic-error sources have been generally treated elsewhere[1] and are not discussed in this paper. Strapdown-application design considerations applicable to the use of the single-degree-of-freedom gyros as typified by the 18 IRIG MOD B[2] are described. The 18 IRIG is a single-degree-of-freedom integrating gyro with a permanent-magnet torque generator and gas-bearing wheel that has been developed at the Massachusetts Institute of Technology (MIT) Instrumentation Laboratory for strapdown-system application. Specifically, torque-generator operational design factors, such as frequency-sensitivity nonlinearities, a.c. torque sensitivity, torque-sensitivity variation with axial, radial, rotational displacement and other environmental inputs are discussed and test results for operation in a digital-ternary-torque-to-balance loop are presented for the 18 IRIG MOD B. Both scale-factor stability and linearity data are shown. Multiple-pulsing characteristics are also reviewed and an active compensation technique to linearize the dynamic response is discussed.

Design of the Integrating Inertial Gyro

The 18 IRIG MOD B design (Fig. 1 and Table 1) is specifically oriented towards a strapdown environment application. The torquer, for example, is compatible with input rates of up to 1 rad/sec. Similarly, the suspension design prevents radial side loading for rates somewhat in excess of 1 rad/sec. A cutaway view of the 18 IRIG is shown in Fig. 1. It has a gas-bearing wheel that rotates at 24,000 rpm and develops an angular momentum of 145,000 g-cm²/sec. A 4-pole, 800-Hz, 2-phase synchronous motor drives the wheel. The wheel and motor structure are mounted in a hermetically sealed cylindrical float. It is pressurized at 1 atm with neon gas. The float is surrounded by a high-density damping fluid and at operating temperature (132°F) it is near neutral buoyancy. Bellows at each end-housing allow for fluid thermal-expansion changes.

An 8-pole-microsyn magnetic suspension at each end of the unit stabilizes the (axial and radial) geometrical relationship between the gyro float and case. At one end of the case is a signal generator (SG) whose output is proportional in magnitude and phase to the angular position of the float about the output axis. Its sensitivity is 20 mv/mrad using an 8-v, 9600-Hz excitation source.

A permanent-magnet torque generator (TG) is at the opposite case end. The permanent-magnet assembly consists of an 8-pole magnet with an armco-iron return path and a torquing coil assembly. The magnet and return path are located on the gyro-case end housing. The coils are mounted on a holder that is attached to the float and are excited through flexible leads. A torque is created on the float about the case output axis that is proportional to the current magnitude applied to the coils. The coils around the magnetic poles are provided to magnetize the permanent magnet. Magnetization is accomplished after the gyro is assembled to eliminate contamination problems that could occur in assembling a magnetized torquer. After magnetizing, it is partly demagnetized with an a.c. voltage. This stabilizes its decay characteristic with time. A magnetic ring located in the end housing on the side of the magnet provides torquer scale-factor temperature compensation.

Wrapped around the gyro case are four nickel-wire-wound temperature sensors for temperature control and monitoring.

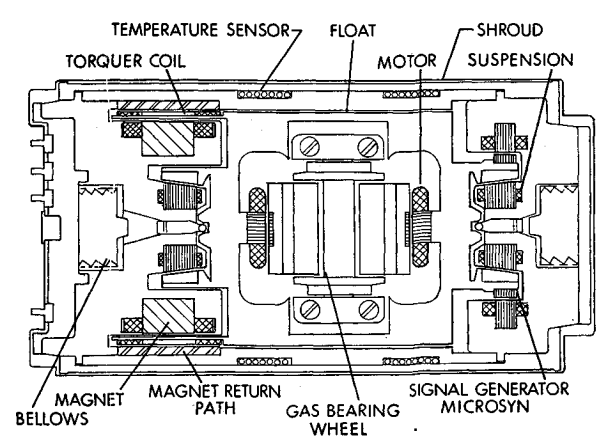

Fig. 1 18 IRIG MOD B simplified cutaway view.

Presented as Paper 69-848 at the AIAA Guidance, Control, and Flight Mechanics Conference, Princeton, N. J., August 18–20, 1969; submitted August 27, 1969; revision received April 17, 1970.

* Director, Apollo Inertial Subsystems Division. Member AIAA.

† Group Leader, Inertial Components.

Table 1 18 IRIG MOD B nominal parameters and operational features

Angular momentum, H	0.145×10^6 g-cm^2/sec
Output axis damping coefficient, C_{OA}	674,000 dyne-cm-sec
Output axis inertia, I_{OA}	225 g-cm^2
Float time constant, $t_f = I_{OA}/C_{OA}$	334 μsec
Transfer function, HS_{SG}/C_{OA}	4.3 mv/mrad
Torquer rate scale factor, SF	1636°/hr-ma
Torquer time constant, $t_{tg} = L/R$	55 μsec
Anisoinertia coefficient $(I_{SA} - I_{IA})/H$	9.6°/hr/(rad/sec)^2
Anisoelastic coefficient, K_{IO}	0.012°/hr-g^2
Float mass unbalance uncertainty, ADIA, ADSRA	0.075°/hr-g

The case is then enclosed in a shroud to provide magnetic shielding and a vacuum envelope to reduce thermal gradients. The unit is approximately 2 in. in diameter, $3\frac{7}{8}$ in. long, and weighs 1.15 lb.

Pulse Torque-to-Balance Operation

The gyro operates in a closed loop where the torques on the float are restrained by control signals to the torque generator. Any rate about the input axis of the gyro produces a torque about its output axis and causes the float to rotate from a null position. The direction and magnitude of the float rotation is sensed by the signal generator. When the SG output voltage reaches a given threshold level, a discriminator provides a positive-or-negative set signal, depending on the polarity of the SG output voltage. These set signals are interrogated at a given clock frequency to switch a control current of fixed amplitude and duration into the positive or negative direction of the torque-generator winding torque. The quality of torque pulses is a very important consideration since each pulse is used by the strapdown algorithm as a corresponding measure of gyro input rate.

For the control-loop mechanization, the principal error source is inaccuracies in the torquer pulse area. For a torque pulse of 75-ma amplitude and 300-μsec width, a scale-factor (SF) error of 1 ppm corresponds to a current-amplitude variation of 75×10^{-6} ma or a pulse-width change of 3×10^{-10} sec.

Multiple-Pulsing Dynamics

An interesting performance characteristic that is not a dynamic error is the multiple-pulsing phenomenon that occurs when the gyro is operated in a pulse torque-to-balance control loop. Multiple-pulsing occurs because of the dynamic storage characteristics of the gyro float time constant.

The gyro float responds to a single torque pulse, which provides a good deal of insight into the lagged response of closed-loop operation at different sampling rates. The response, as plotted in Fig. 2, shows that only a small percentage of he total float motion to a single fixed-magnitude torquing pulse occurs in the first sampling period. For example, at a 9600-pulse/sec interrogation rate the float has only begun to move when the torque pulse is turned off and has gone 11% of its commanded travel when the next torque-loop interrogation sample takes place. At the 3200-pulse/sec interrogation rate approximately 34% of the travel has occurred by the time the next sample is made.

Clearly, at 9600-pulse/sec closed-loop operation, a W_{IA} angular rate about the gyro input axis that is in excess of 11% of the torque-loop, full-on, rate-scaling capability will result in some form of multiple-torque pulsing. For example, consider an initial condition in which a steady-state W_{IA} is such that the float travel in a sampling period is slightly in excess of 11%. At sampling time (assume the float crosses over the torquing threshold exactly at a control-loop sampling point), a restraining torque-command pulse is issued. The float

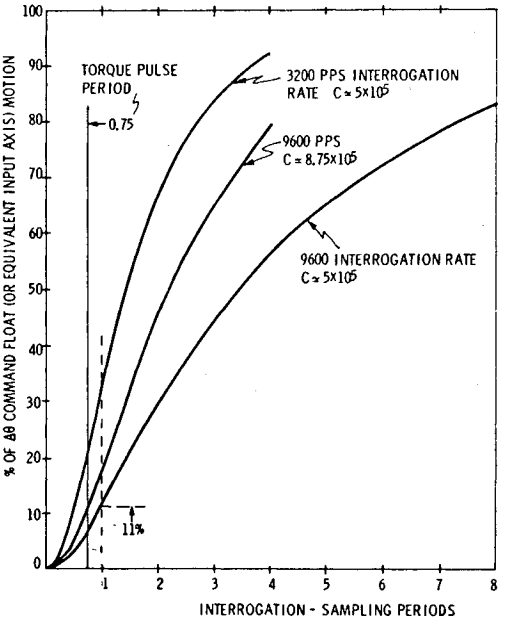

Fig. 2 Normalized gyro response to a single torque pulse command.

operates such that the steady-state input and the pulse command are summed. Thus, at the next sampling interval the float is still outside the threshold and another torque pulse is commanded. The effect over these two sampling periods has been to command two $\Delta\theta$ increments in response to an input slightly in excess of one $\Delta\theta$. For the next few sampling periods the float response to the two successive torque pulses dominate and no further output pulses will occur. Then, dependent upon the threshold cross-over relationship with the sampler, another pulse burst may occur. The average indicated rate is correct but a pattern of pulse on-and-off bursts may occur.

A compensation technique has been suggested by Lory[3] for a pulse-rebalance loop to minimize moding and multiple pulsing. This technique models the gyro so that a response of the gyro to the actual pulses issued is continuously developed. This information is then used to anticipate the float motion response to pulse commands and linearize the torque-loop output response. That is, a compensating signal based on the computed float response to each torque pulse is compared to the actual gyro SG status, thereby accounting for float-motion delays and eliminating unnecessary multiple pulsing.

The effectiveness of this compensation technique is illustrated by considering the response of a gyro with an uncompensated and compensated ternary pulse rebalance loop after an initial float displacement of five-pulse quanta (Fig. 3). The uncompensated system exhibits a mode pattern whereas the compensated system settles after a five-pulse output. This figure illustrates how compensating the system has linearized its response and allowed operation with a tighter dead band without moding.

Gyro Torque Generator Design Factors

As previously noted, it is the high-rate torque-to-balance capability with minimum adverse performance effects that is the essential requirement for strapdown-gyro utilization. This section discusses some of the over-all considerations associated with the torquer design and its utilization in a strapdown torque-to-balance control loop.

The 18 IRIG employs a permanent-magnet torque generator as opposed to the square-law torquer used in the Apollo Gyro. As such, it is a linear device and (apart from non-

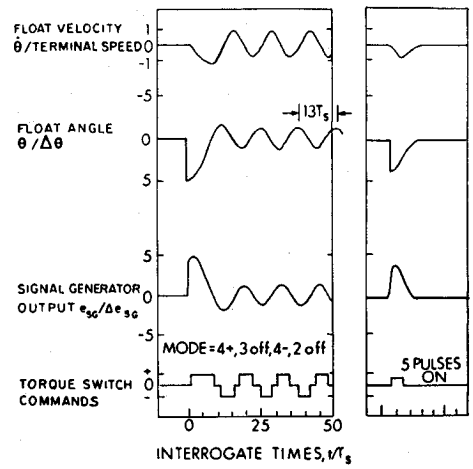

Fig. 3 Responses of uncompensated (left) and compensated (right) systems to initial condition $\theta = 5\Delta\theta$; deadband = $\pm \frac{3}{4} \Delta\theta$.

ideal features) the magnetic stability and torquer scale-factor errors associated with current-transient rise and decay characteristics are eliminated.

With respect to the torquer, a variety of sensitivities associated with the torquer-assembly geometry and materials as well as environmental inputs to the gyro must be considered. Some of the sensitivities that are briefly described here are 1) gyro rotational float angle, 2) float radial and axial positions, 3) magnetic material interaction, and 4) thermal inputs.

With respect to the geometry of the torquer, scale-factor (torque-sensitivity) changes occur for different float rotational angles (coil-magnet pole orientation). In the torque-to-balance operational mode the float angle is maintained within the threshold level (quantization) of the ternary control loop which is centered about the SG null. Sensitivity changes can be minimized by reducing misalignments between the SG null position and the TG maximum sensitivity position. Beyond this provision the design itself must allow operation in the ternary deadzone region without exhibiting appreciable torquer sensitivity changes. For a high-performance strapdown application a desirable budget of torquer SF sensitivity uncertainties due to this effect would be 2 ppm.

Float radial displacement occurs due to an angular rate about the gyro output axis. This rate operating on the angular momentum of the wheel causes a torque about the input axis. This torque is resisted by the magnetic suspension. The suspension must be adequate to prevent radial displacement to a jewel extreme under angular rates of up to 1 rad/sec (the maximum rate for which strapdown system design has been considered at our laboratory). A budget for torquer-sensitivity changes resulting from the radial float motion due to the rate about OA of less than 25 ppm for rates up to 1 rad/sec is considered desirable.

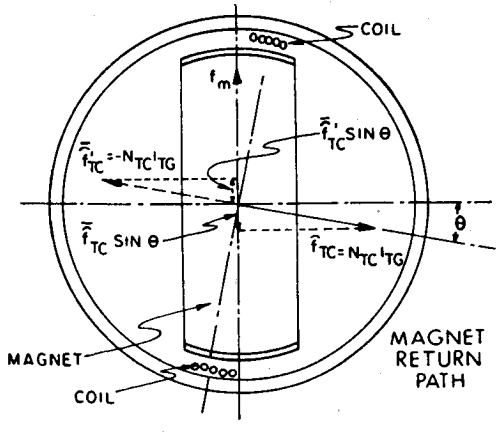

Fig. 4 Torquer coil reaction effect for 2-pole PM torque generator.

Linear acceleration input will also cause radial and axial displacements that are proportional to the difference between the operating and the unit flotation temperature. Under 10 g's of linear acceleration and a 2°F flotation-temperature error, the axial or radial displacement that could result should cause changes in torquer sensitivity of less than 50 ppm.

Magnetic-material interaction on the assembly can adversely influence instrument-torquer sensitivity and basic performance stability. For example, any magnetic material on the float that is in the vicinity of the magnet can interact to yield torque uncertainties in the BD drift terms. It would be desirable to assure that such influences would account for less than 0.2-meru BD uncertainty. Similarly, magnetic influences in the torquer assembly can contribute to errors in scale-factor linearity and stability. System studies have shown that, for typical spacecraft operations, a desirable design objective would correspond to total SF linearity of 50-ppm over the 0.001-to-0.4-rad/sec range. From 0.4-to-1 rad/sec linearity, of 100-ppm would appear to be adequate. SF stability of 20 ppm would represent a reasonable performance objective.

Temperature sensitivity represents a trade-off between temperature control-loop capabilities and internal magnet-compensation technique complexities. Temperature control to within ±0.1°F is attainable and a torquer sensitivity of 10 ppm/°F appears to be a reasonable objective.

In light of these considerations and performance objectives, the sensitivities of the inertial 18 IRIG development units were evaluated. Several interesting problem areas were uncovered and design solutions generated. After providing theoretical background, the remaining discussion will review these areas.

Rotational Float-Angle Sensitivity

In an actual instrument the torque generated differs when the same current is applied in opposite directions through the torquer coil. The torque difference may be explained by noting that the SG null position and the TG maximum torque-sensitivity positions are not perfectly coincident. Thus, if the gyro is operated with the float at its SG null, the torquer is not necessarily at its optimum position with respect to the magnet. Figure 4 illustrates this condition. A single coil is shown relative to a two-pole magnet. The plane of the coil makes an angle θ with the plane of the permanent magnet. For the direction of current in the coil as shown, the MMF of the permanent magnet (f_m) is decreased by a component of the coil MMF of magnitude ($f_{TC} \sin\theta$). If the coil current is reversed, the component of MMF of the torquer coil f_{TC} adds to the permanent-magnet field. This results in a torque difference between cw and ccw torquing that is proportional to the angle between the plane of the permanent magnet and coil (θ). For θ equal to zero, the cw and ccw torquer scale factors would be equal. In the gyro, this effect will cause a ΔSF change proportional to unit float angle about the output axis. This difference between positive and negative scale factor, called ΔSF, is given by the following relationship:

$$\Delta SF = N_{TC} I_{TG} \theta / F_M \qquad (1)$$

where N_{TC} = torquer coil turns, I_{TG} = torquer current (ma), F_M = permanent-magnet MMF (ma-turns), and θ = angular misalignment between torquing coil and permanent-magnet pole (rad).

Similarly, if an a.c. current is fed to the coil, an output torque will result that is proportional to the angle θ and to the magnitude of the current. This a.c. torquer sensitivity

can be used in the assembly of the instrument to minimize the cw and ccw torquing scale-factor difference.

Early in the program, large torquer sensitivities with changes in rotational, radial, and axial float motion were evidenced. The problem was traced to the magnet casting. It was found that the magnet casting could not be fabricated to accurately locate the maximum flux density at the center of each mechanical pole. A composite-magnet structure was then developed that consists of a ring upon which salient poles are accurately fixtured and adhesively attached.

Figure 5 illustrates the relative difference in torque-generator scale-factor variation with the float angular displacement from its electrical null position for typical cast and composite magnet designs. Similarly, scale-factor radial-position sensitivity is shown in Fig. 6. In this curve scale-factor is shown with the rotors displaced radially along IA and SA from the stator center. SF is measured for each of these displacements. These figures clearly illustrate the marked improvements in the scale-factor sensitivity of the composite magnet.

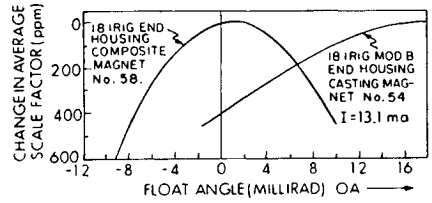

Fig. 5 TG scale factor sensitivity vs float angle.

Magnetic-Material Interaction

The two basic material-interaction problems encountered were stop-bias hysteresis and eddy-current sensitivities. Stop-bias hysteresis is the term used to describe instrument-bias sensitivities that result when magnetic materials are present on the float in the vicinity of the permanent magnet. These magnetic particles assume a domain orientation that stays fixed until their orientation relative to the magnet changes. For example, during test, if the float moves towards a rotational stop (gyro is not held at SG null), the magnetic particles assume a new random domain orientation. This causes a change in the total reaction torque on the float. For this instrument the cause of the stop-bias hysteresis was associated with the coil-holder material iron content. The holder on this gyro was fabricated from I-400-grade beryllium which has an allowable iron impurity content of 0.5% maximum. The coil holder is now fabricated from high-purity beryllium oxide and only OFHC copper wire drawn through nonmetallic dies is used for the coils. Further, all holders are tested for stop-bias sensitivity prior to assembly in a gyro; the effect has been significantly reduced.

It is interesting to note that a similar experience occurred with an accelerometer that employs a potted torquing-coil assembly. Similar erratic performance was observed and, in this case, traced to magnetic particles dispersed throughout the potting compound. It was discovered that these particles were introduced during the manufacture and processing of the compound filler material.

The second nonlinear effect resulted from eddy currents that were induced in the torquer-coil holder when the gyro was operated in the pulse-rebalance type of control loop. In this loop, pulses of current are applied to the torquer coil at a rate that is proportional to the input rotational rate sensed by the gyro. For the initial beryllium coil holder it was noted that eddy currents were being induced in the coil holder when current pulses were applied. These eddy currents then interact to affect the coil loading characteristics and torquer sensitivity. For example, Fig. 7 shows the variation in torquer inductance for a beryllium torquing-coil support and one made from a nonmetallic material (Bacon Ind. P-20 potting compound) with both a laminated and solid return path.

In addition to impedance variation with frequency, the reaction-torque characteristics for a rotational float offset for an a.c. current also exhibited a nonlinear characteristic with frequency as illustrated in Fig. 8. In a similar test conducted on a titanium coil support the various curves effectively merged into a single line. The major difference is in the level of induced eddy currents in the holder; beryllium is a fairly good electrical conductor (4.3 μohm-cm), whereas titanium is not (176 μohm-cm).

Both of the effects described influence the scaling characteristics of the gyro operating in the torque-to-balance loop. For the ternary control loop, the pulse rate and moding patterns are functions of the applied angular-input rate. The frequency content of the torquing current is therefore directly related to the input rate and, thus, the result is a scale-factor nonlinearity. The inductance and resistance changes directly influence the performance of the torque-current-magnitude control loop which is band-width limited. Thus it is evident that beryllium is not an ideal selection for a torque-coil support for a gyro used in a strapdown application.

It should be noted that beryllium is commonly used for gyro floats because of its high structural stability and low density. Its initial selection, therefore, for a coil holder that mounts to the float was evolutionary in nature since it simplifies balancing and material thermal-gradient stability.

Other materials supports are being investigated to minimize eddy-current effects. Nonconductive designs of plastic (potted assembly) and ceramic materials have been developed. The present 18 IRIG design, for example, uses beryllium-oxide ceramic.

Torque-Generator Power

A major system-design consideration is the torque-generator scale factor (dyn-cm/ma). If a gyro is to operate in the torque-to-balance mode, clearly the power level required to accommodate a one-radian-per-second capability must be realistic. Further, the power dissipated in the coil must be such that thermal-gradient unbalances (affecting basic gyro-drift performance) and SF uncertainties are not generated.

Since the coil design is essentially restricted by volumetric limitations (gap size and pole dimensions), resistance tends to be fixed by the physical necessity of filling the available

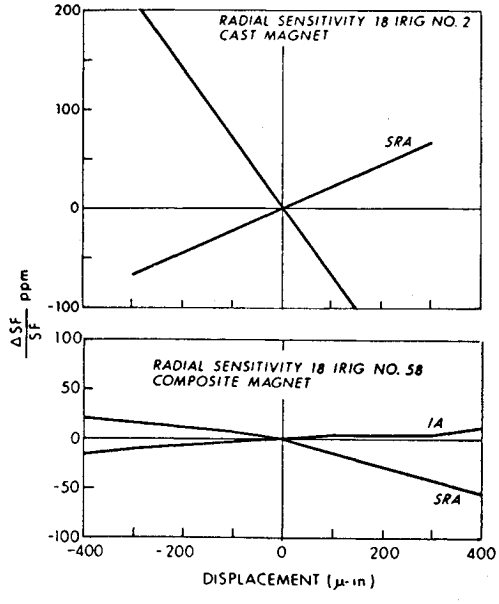

Fig. 6 Scale factor-radial sensitivity.

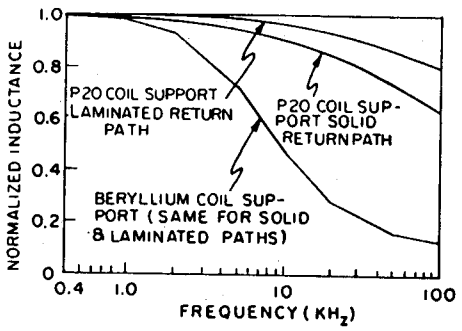

Fig. 7 Normalized frequency sensitivity plastic vs beryllium coil holder.

space with as many turns as possible. One optimizing design feature is to locate the coil holder at the maximum possible outside dimension of the float. To achieve this on the 18 IRIG, an inside-out magnet structure was designed. (Note in Fig. 1 that the magnet is encircled by the coil and its return is an outside diameter located in the case structure.)

After the structural-design parameters have been optimized, remaining improvements can only be achieved by increasing the gap flux density via magnet-material selection. It is interesting to note that increasing the gap flux density also yields the added advantage of reducing SF difference sensitivities, etc. Studies were therefore conducted to optimize the material selection for the magnet. One interesting development that has been incorporated in the gyro design was the use of different materials for the magnet's ring and pole structures. This was possible because of the composite nature of the design. Specifically, initial magnets were fabricated of Alnico V material and a significant improvement was achieved by using Alnico V for the ring and Alnico IX for the pole pieces. The relative improvement is shown in Table 2.

It is important to emphasize that the absolute stability of the flux density determines the practicality of application of a permanent magnet gyro torquer to an actual system. Tests conducted on these designs have repeatedly demonstrated a torquer magnet 30-ppm/decade logarithmic decay characteristic. Thus, after an initial magnetization and stabilizing period (approximately 90 days), the total long-term decay is less than 10 ppm per year.

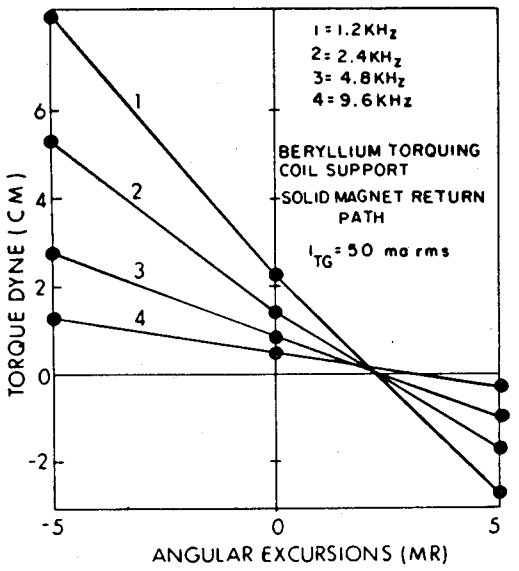

Fig. 8 Reaction torque vs angle and frequency.

Table 2 Torque parameter changes due to pole piece material change (Ring material Alnico V)

Torquer parameters	Alnico V poles	Alnico IX poles
Flux density stabilized (B_g)	1600 gauss	2380 gauss
Generator sensitivity (S_{tg})	775 dyne-cm/ma	1150 dyne-cm/ma
Power at 150,000 dyne-cm (1 rad/sec)	5.7 w	2.59 w
Scale factor difference at 1 rad/sec (ΔSF)	110 ppm/mrad	50 ppm/mrad

Signal Generator Noise

In the strapdown implementation $\Delta\theta$ quantization in the range of 1 to 6 arc-sec has frequently been discussed for optimization of attitude-maintenance performance. For the 18 IRIG this corresponds to a torque-loop-discriminator torque command that corresponds to an SG output of 30–180 μV. For satisfactory instrument torque-to-balance loop mechanization discernible SG signal-to-noise ratios are necessary.

Within bounds, some of the major noise sources arising from wheel-power pickup (800 Hz) can generally be filtered in a preamplifier prior to transmission to the torque-loop level discriminator. In evaluation testing we typically employed a 9.6-kHz $\pm$3-kHz band-pass filter; narrower band-pass limits would hazard system performance since it would affect the integrity of data transmission to the system algorithm computer.

Within this band-pass region any erroneous sources of SG signal modulation result in erroneous torquing of the gyro. One modulation source anticipated corresponds to the 400-rad/sec rotation rate of the wheel; i.e., wheel vibration directly inducing float motion. The amplitude of this modulation is reduced by precise dynamic balancing of the wheel. Generally, tests have shown that with the 18 IRIG gas-bearing design this level of modulation can be held to one microvolt at the SG output. It was discovered, however, that sizable (15-μV) modulation side bands existed at $\pm$1600 Hz. This was traced to magnetic coupling in gyro connector pins caused by motor current. The connector-pin material (Kovar) is commonly used in gyro fabrication for hermetic sealing of the case in that its thermal expansion coefficient matches the glass seal. Unfortunately, it possesses magnetic properties and, as a result of these findings, a suitable nonmagnetic pin was phased into the design. A problem of this nature would not be of any consequence in a gimbal-mounted gyro application. It serves to illustrate another strapdown-application design factor.

Gyro Evaluation Testing

Five of the initial developmental 18 IRIGs have undergone extensive strapdown evaluation. Initial torquer evaluation testing was conducted with precise d.c.-current-level inputs and was intended to define a baseline for sensitivities with respect to float angle, radial and axial displacement, and temperature. The second phase was testing in a ternary pulse-torque-to balance control loop. In these tests scale-factor stability and linearity with various test rates and torquing parameters were investigated. All tests were conducted on a precision air-bearing test table that could be either operated in a gyro servo mode or driven at precise-angular input rates (15°/hr to 600°/sec), and a band-pass pre-amplifier mounted close to the gyro test block was used to provide noise and 800-Hz wheel-power filtering. It was reassuring to note that the measured sensitivities fall within the range

of design-error budgests (discussed previously) that were defined on the basis of system-performance objectives.

Torquer sensitivity to rotational float angle θ was determined for various d.c.-current levels applied to the torquer with the test table operating in a servo mode. Table rates were determined using the table inductosyn readout. The first assembled unit that was evaluated showed a larger torquer sensitivity with rotational angle because of improper SG-to-TG alignment as illustrated by the average SF plot in Fig. 9. Note that the average SF sensitivity about the zero float-angle position (corresponding to the SG null) is on the order of 70 ppm/mrad and that the point of maximum SF corresponds to approximately +5 mrad. As explained previously, optimum performance is achieved when the gyro alignment is such that the SG null is coincident with the TG maximum-torque position. The test results, therefore, indicate an SG-to-TG misalignment on this unit was on the order of 5 mr which also accounts for the relatively large plus-to-minus SF difference (ΔSF) observed (200 ppm) in closed-loop operation. Subsequent tests on an improved unit aligned using a technique that is based on the a.c.-current torquer sensitivity (see previous rotational float-angle discussion) demonstrated a reduction of the average SF sensitivity about the SG null to 6 ppm/mr and a reduction in the closed-loop ΔSF to approximately 25 ppm.

The measured temperature sensitivity of the torquer was 16 ppm/°F although a design goal of 10 ppm/°F was initially postulated. This level of scale-factor variations is not a problem, since thermal control to within 0.1°F is anticipated.

Average scale-factor sensitivity to radial displacement along IA and SRA was less than 10 ppm for a radial displacement of 400 μ in. A rate about the gyro output axis of more than 1-rad/sec would cause radial displacements of this magnitude. With axial displacement changes of 250 μ in., the torquer sensitivity changes by less than 50 ppm. This axial displacement would occur for a $2\frac{1}{2}$°F floatation error and 10 g's acting along the output axis.

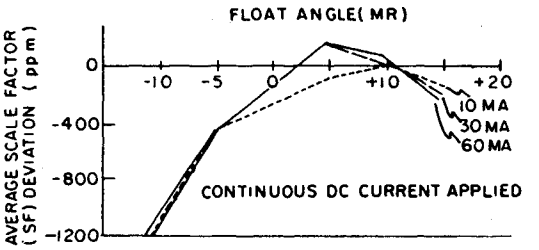

Fig. 9 Unit 411, 18 MOD B scale factor vs float angle.

Torque-to-Balance Testing

Test Electronics

The instrument was tested employing a ternary-pulse-restrained torque-to-balance control loop. "Ternary" is used in the sense there are three distinct torquing states: positive, negative, or zero torque. The simplified mechanical switching schematic, Fig. 10 (semiconductor switches are actually used), helps illustrate ternary control and some of the subtleties of the test electronics. The switch status is shown in the positive-torque mode. Note the torquing polarity is set by an "H" switch that feeds current into the plus-or-minus direction of the torquer winding. Switch S_5 operates so that current flows through either a dummy load or the torquer winding.

The dummy load is a noninductively wound heater (approximately the same resistance as the torquer winding) that is located on the alignment mounting hardware that attaches to the TG end of the gyro. Thus, S_5 not only turns on the command torquing (set position) but also is mechanized to maintain a thermal balance in the reset position. In addition, regardless of the torque-command state, approximately the same current is fed into the scale-factor resistor. The scale-factor voltage is compared with a precision-voltage reference in the input stage of a high-gain d.c. amplifier. The amplifier is part of the d.c. control loop that maintains a precise fixed-current level. Note also that an RC compensation network is connected across the torquer. It functions to tune the torquer so that the load seen by the switches and current source is purely resistive.

The turn-on and turn-off torque occurs only at specific switch set-and-reset pulse times respectively. For the test configuration that was used, a switch set-and-reset pulse is issued in each (interrogation) clock cycle. The reset pulse precedes the switch pulse so that a torque-off command exists in each clock cycle. Thus, current is applied to the torquer as pulses. The average applied restraining force is a function of the number of torque pulses applied during the measurement period, and the pulse rate corresponds to the applied input angular rate.

Multiple Pulsing

During testing in the closed-loop pulse-torque-to-balance mode multiple-pulsing was observed. Without the linearizing compensation scheme described previously, the gyro float dynamics caused the torque-loop to cyclicly torque in pulse bursts for input rates in excess of approximately 1.5°/sec for a 9600-pps interrogation sampling rate. This phenomenon directly limits the effective $\Delta\theta$ quantization magnitude if one considers a DDA type of strapdown-system computational configuration. A whole-number computational scheme is less sensitive to this effect. For example, in computer simulation, for a 15°/sec maximum system-rate scaling with the 9600-pps interrogation, pulse-bursting of 3 torque pulses on and 12 off was predicted for a 3°/sec rate input. On gyro #411 a 3-on 12-off bursting pattern was observed in the region of 2.8°/sec. Although the average pulse rate corresponds to 20% of maximum rate input scaling, the preferred response is a linear pulse cycle of 1-on 4-off. At low rates a "double-pulsing" effect was noted. That is, an additional erroneous pulse of the same polarity would occur immediately following a normal torque command. The additional pulse does not drive the float through the electron-

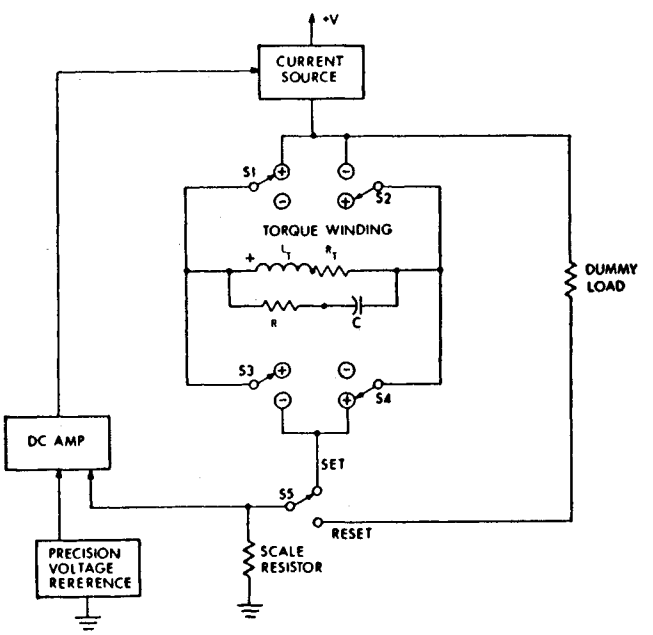

Fig. 10 Ternary pulse torque switching.

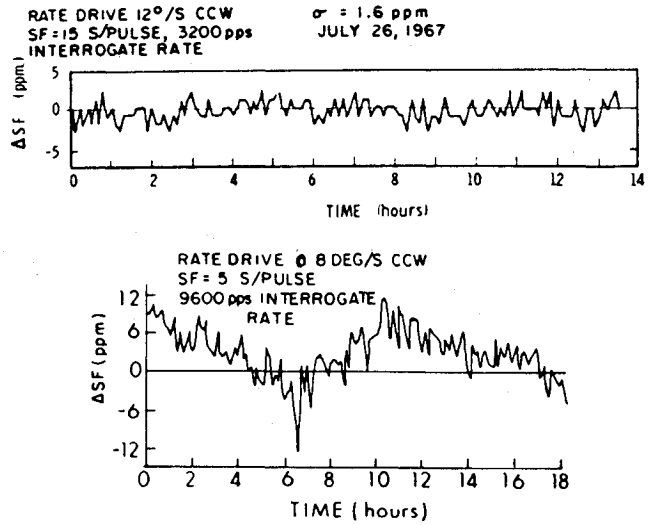

Fig. 11 Pulse torque SF stability 18 IRIG MOD B 411.

ics ternary-control dead zone but does represent a source of measurement error. This double-pulsing occurred randomly and was traced to the presence of noise at the SG induced by the torque-current changes at the TG. Although this effect was minimized by changes in the relative spacing of the reset-and-set pulses in the torque electronics, it could not be completely eliminated at high interrogation sampling rates with the test electronics used. (This finding precipitated a torque-loop logical-design change in interrogation timing that has been phased into current systems.)

Pulse-Torque Test Results

The torquer frequency sensitivity, resulting from the coil-holder eddy-currents, combined with multiple-pulsing, yield varying degrees of measurement and performance instabilities. These are evidenced during pulse-torque-to-balance scale-factor stability and linearity testing. As discussed previously, both multiple-pulsing and eddy-current frequency sensitivities are more pronounced at higher control-loop interrogation rates. Thus, superior SF stability and linearity was always exhibited at 3200-pps as opposed to operation at 9600-pps. Fig. 11a shows a 13-hr scale-factor stability run on a test unit at a 3200-pps interrogation rate. A total excursion of 5 ppm was obtained. The best 9600-cps interrogation stability test run on this unit (Fig. 11b) resulted in excursions on the order of 15 ppm with peaks of 25 ppm.

Torque-to-balance SF-linearity testing was conducted at 3200-, 4800-, and 9600-pps interrogation rates. During testing the torquer impedance variation effects caused by eddy currents were reflected by an inability to resistively tune the torquer coil with a single RC network. [Recall that in the discussion of eddy-current effects the coil impedance due to the beryllium holder was shown to be frequency dependent (Fig. 8).] This effect resulted in extremely poor SF linearity for input angular rates. The SF nonlinearity was primarily due to the inability of the torque-to-balance electronics' precision-current control loop to accommodate the wide impedance-load variations resulting from the difference pulse-torquing rate-frequency characteristics. This problem was experimentally resolved by cascading three parallel RC

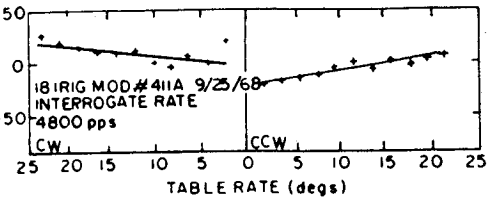

Fig. 12 Scale factor linearity.

networks (time constants of approximately 114, 10, and 3 μsec) that closely matched the impedance frequency-dependent characteristics of the torquer coil assembly. Linearities obtained for the gyro-torque-loop operation were on the order of 100 ppm and 200 ppm for 3200-pps and 9600-pps interrogation rates, respectively, over an input range of 1° to 10°/sec. This performance was generally achieved with the first 4 developmental units that incorporated a low-SF torquer, beryllium coil holder and featured varying degrees of SG-to-TG alignments (1 to 5 mrad). The last instrument evaluated (#411A) incorporated a high-SF torquer magnet and better than a one-milliradian alignment accuracy. For this instrument, linearity performance on the order of 50 ppm over an extended test range of ±25°/sec was achieved (Fig. 12). The remaining nonlinearities are attributable to the eddy-current reaction-torque sensitivities, geometric displacement sensitivities, and basic torque-loop performance. The remaining eddy-current effects will be eliminated in future instruments that incorporate the beryllium-oxide coil holder.

Conclusion

The discussion has shown that the design of a single-degree-of-freedom gyroscope for a strapdown system represents a departure from the standard gimbal-mounted gyro design. In addition to the application design factors (such as maximum torquer-rate capability and suspension stiffness) necessitated by a strapdown environment, other factors must be considered. Some subtle effects of signal-generator-to-torque-generator alignment, coil-holder material selection, signal-to-noise ratio, and scale-factor change due to dynamic inputs must be evaluated. The development of the 18 IRIG has shown that these design factors can be evaluated and successfully resolved. Relatively high-performance torquer-scale-factor stability and linearity are attainable. Therefore, an inertial-grade strapdown-system instrument mechanization is entirely feasible for spacecraft environmental applications.

References

[1] Inertial Subsystem Group, *Control, Guidance and Navigation for Advanced Manned Missions, Report R-600*, Vol. IV (Structure Mounted Studies), Instrumentation Lab., Massachusetts Institute of Technology, Cambridge, Mass., Sept. 1968.

[2] Aronson, J. H. et al., "18 IRIG MOD B Final Report, December 1965–August 1968," Internal Memo FBM/IC 021, Instrumentation Lab., Massachusetts Institute of Technology, Cambridge, Mass.

[3] Lory, C. B., *Compensation of Pulse Rebalanced Inertial Instruments, T-495*, Instrumentation Lab., Massachusetts Institute of Technology, Cambridge, Mass., Jan. 1968.